# Nuclear-spin relaxation in the boson-fermion model of superconductivity

R. Friedberg and T. D. Lee
*Columbia University, New York, New York 10027*

H. C. Ren
*Rockefeller University, New York, New York 10021*
(Received 30 August 1991)

The nuclear-spin-relaxation rates in high-$T_c$ cupric oxide superconductors are calculated from the (phenomenological) boson-fermion model. It is shown that the model is consistent with the experimental data for both Cu and O sites, in the superconducting as well as in the normal phase.

## I. HAMILTONIAN

NMR measurements[1,2] of the nuclear-spin-relaxation rate $T_1^{-1}$ on the high-$T_c$ superconductors show a superconducting phase temperature $T$ dependence different from that given by the standard BCS theory.[3] It has been suggested[1] that this deviation from the normal behavior could be due to a $d$-wave pairing.[3] In this paper, we wish to analyze the same phenomenon in the context of the boson-fermion model (the $s$-channel theory) of superconductivity.[4,5] We find the observed behavior to be consistent with the hypothesis of having a nonspherically symmetric internal resonant wave function of the $\phi$ quantum, either a $p$ wave or a $d$ wave.

In addition, the normal-phase behavior of $T_1^{-1}$ at the Cu sites is found to be different from that at the O sites,[1,2] with the Korringa product [defined to be $(T_1T)^{-1}$] decreasing with increasing temperature for the Cu sites, but approximately constant for the O sites. This is difficult to understand if there is only a single fermion component, as in the BCS theory. In the boson-fermion model, as we shall see, the bosons and fermions give different temperature variations of the Korringa product. The observed difference can be phenomenologically accounted for by assuming different probabilities for finding bosons at the Cu and O sites.

To gain a perspective on this approach, we begin with a brief summary of the model: The small coherence length[6] in the high-$T_c$ superconductors has led to the assumptions that the pair-state can be represented phenomenologically by a local quantum bosonic field $\phi(\mathbf{r})$ and that the dominant underlying reaction of superconductivity is the $s$-channel process

$$2e \to \phi \to 2e \ ; \tag{1.1}$$

this replaces the $t$-channel reaction

$$2e \to 2e + \text{phonon (or other excitation)} \to 2e \tag{1.2}$$

in the BCS theory. The strong Coulomb repulsion between $2e$ makes an individual $\phi$ unstable:

$$\phi \to e(\nu) + e(\nu) \ , \tag{1.3}$$

where $\nu$ denotes the energy of $e$ in the rest frame of $\phi$. However, because of the exclusion principle, such a $\phi$ becomes stable when there is a Fermi sea of $e$ of top energy

$$(2m_f)^{-1}k_F^2 = \nu \ , \tag{1.4}$$

with $k_F$ being the corresponding momentum and $m_f$ the fermion mass. The coexistence of these two types of carriers, bosons and fermions, is the main feature of the $s$-channel theory.

We concentrate on the Fermi contact interaction Hamiltonian between the nuclear spin $\mathbf{I}$ at $\mathbf{r}_N$ and the spin associated with the electron field

$$\psi = \begin{bmatrix} \psi_\uparrow(\mathbf{r}_e) \\ \psi_\downarrow(\mathbf{r}_e) \end{bmatrix} , \tag{1.5}$$

at $\mathbf{r}_e$ (with $\uparrow$ and $\downarrow$ denoting the spin indices):

$$H = -\tfrac{1}{3}\gamma_e\gamma_N\psi^\dagger(\mathbf{r}_N)\boldsymbol{\sigma}\psi(\mathbf{r}_N)\cdot\mathbf{I} \ , \tag{1.6}$$

where $\boldsymbol{\sigma}$ is the Pauli spin matrix, $\frac{1}{2}\gamma_e\boldsymbol{\sigma}$ denotes the magnetic moment of $e$, and $\gamma_N\mathbf{I}$ that of the nucleus. This interaction applies to both the "bound" electrons in the resonance state $\phi$ and the "free" electron field $\psi_f$, whose Fourier expansion can be written as

$$\psi_f(\mathbf{r}) = \sum_{\mathbf{k}} \frac{1}{\sqrt{\Omega}} \begin{bmatrix} a_{\mathbf{k}\uparrow} \\ a_{\mathbf{k}\downarrow} \end{bmatrix} e^{i\mathbf{k}\cdot\mathbf{r}} \ . \tag{1.7}$$

Here, $\Omega$ is the volume of the system, and the subscript $f$ emphasizes the difference between $\psi$ of (1.5) and the phenomenological fermion field $\psi_f$ [see Eqs. (1.13) and (1.14) below]; $a_{\mathbf{k}\uparrow}$ and $a_{\mathbf{k}\downarrow}$ denote the annihilation operators of $\psi_f$. As we shall see, the effects of the "bound" and "free" electrons on the nuclear-spin-relaxation rate are quite different.

Take the $z$ axis to be perpendicular to the $CuO_2$ planes, and assume that the resonance $\phi$ is in a $2e$ channel with antiparallel spins $\downarrow\uparrow$. The transition in which the $z$ component of nuclear spin decreases,

$$I_z \to I_z - 1 \ , \tag{1.8}$$

can be caused by changing either the "free" electron spin or the "bound" one. In the latter case, the switching of the "bound" electron spin from ↓ to ↑ puts the final $2e$ in the ↑↑ channel. Since there is no resonance in that channel, we have the boson-dissociation reaction

$$\phi(\mathbf{q})+I_z \rightarrow e_\uparrow(\mathbf{p}_1)+e_\uparrow(\mathbf{p}_2)+(I_z-1)\ , \tag{1.9}$$

where $\phi(\mathbf{q})$ denotes a $\phi$ quantum with momentum $\mathbf{q}$, and $e_\uparrow(\mathbf{p}_1)$ or $e_\uparrow(\mathbf{p}_2)$, of momentum $\mathbf{p}_1$, or $\mathbf{p}_2$, refers to the "free" electron described by $\psi_f$ of (1.7). Because $\phi$ is a resonant state (not a bound state), this reaction is exothermic.

The effective Hamiltonian for reaction (1.8) can be written as

$$\begin{aligned} H_{\text{eff}} = & -\frac{1}{3\Omega} I_- \gamma_e \gamma_N \sum_{\mathbf{p}_1,\mathbf{p}_2} e^{i(\mathbf{p}_1-\mathbf{p}_2)\cdot \mathbf{r}_N} a^\dagger_{\mathbf{p}_2\uparrow} a_{\mathbf{p}_1\downarrow} \\ & + (2\Omega^{1/2})^{-1} \sum_{\mathbf{p}_1,\mathbf{p}_2} \mathcal{M}_{\mathbf{p}_1\mathbf{p}_2\mathbf{q}} e^{i(\mathbf{q}-\mathbf{p}_1-\mathbf{p}_2)\cdot\mathbf{r}_N} \\ & \times (a^\dagger_{p_1\uparrow} a^\dagger_{p_2\uparrow} b_\mathbf{q} - b^\dagger_{-\mathbf{q}} a_{-\mathbf{p}_2\downarrow} a_{-\mathbf{p}_1\downarrow})\ , \end{aligned} \tag{1.10}$$

where the first term is due to the "free" electrons [Fig. 1(a)], the remaining terms are due to the "bound" electrons in $\phi$ [Figs. 1(b) and 1(c)] and its inverse processes [Figs. 1(d) and 1(e)],

$$\begin{aligned} I_- &\equiv \langle I_z-1 | I_x - iI_y | I_z \rangle \\ &= [I(I+1)-I_z(I_z-1)]^{1/2} \end{aligned} \tag{1.11}$$

is the nuclear matrix element, $b_\mathbf{q}$ is the annihilation operator related to the boson field by

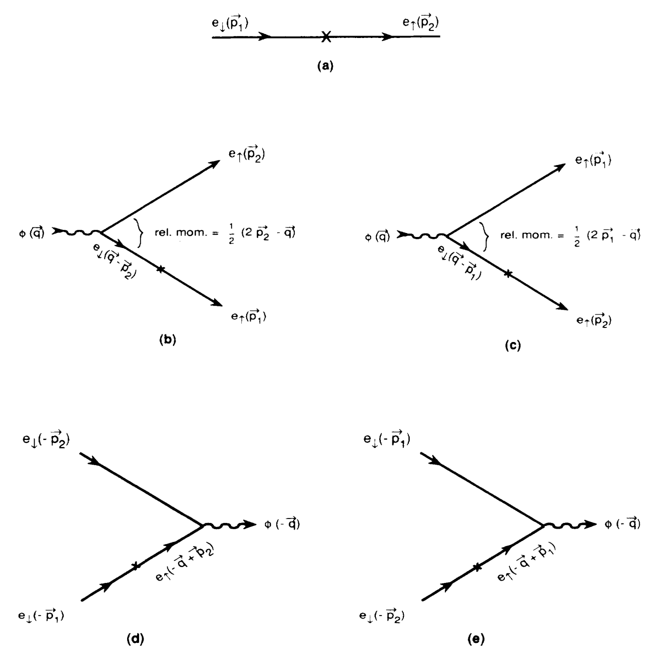

FIG. 1. All the processes contributing to reaction (1.8) in the normal phase, where $e_\sigma(\mathbf{p})$ denotes an electron of momentum $\mathbf{p}$ and spin $\sigma$ $(=\uparrow,\downarrow)$, $\phi(\mathbf{q})$ denotes a boson of momentum $\mathbf{q}$, and the cross represents the action of the contact interaction (1.6). The rates of these processes are given by (3.2)–(3.6).

$$\phi(\mathbf{r})=\sum_q \frac{1}{\sqrt{\Omega}} b_\mathbf{q} e^{i\mathbf{q}\cdot\mathbf{r}}\ , \tag{1.12}$$

and the coefficient $\mathcal{M}_{\mathbf{p}_1\mathbf{p}_2\mathbf{q}}$ is associated with the internal wave function of the $\phi$ quantum, which is to be discussed in the next section. [The relative sign between the two terms $a^\dagger a^\dagger b$ and $aab^\dagger$ in (1.10) has been chosen negative in order to conform with the desired reality condition (2.6) on the bosonic internal wave function. See (2.11) and remark (2) at the end of Sec. II.]

In this model, the total charge density of both the "free" and the "bound" electrons (in units of $e$) is

$$\psi^\dagger\psi = n_f + 2n_b\ , \tag{1.13}$$

with

$$n_f = \psi_f^\dagger \psi_f \quad \text{and} \quad n_b = \phi^\dagger \phi\ . \tag{1.14}$$

As shown in Ref. 5, for applications to high-$T_c$ superconductors, depending on the doping, the expectation value of $n_b$ can be much larger than that of $n_f$. Therefore, the bosonic component plays an important role.

In the $s$-channel theory, below the critical temperature $T_c$, both bosons and fermions are superconducting. The superfluidity of the bosons is due to Bose-Einstein condensation. Therefore, it exhibits a characteristic two-fluid behavior, like He II. The dominance of the bosonic component would naturally lead to qualitative agreements with the NMR measurements, as well as more recent infrared conductivity experiments.[7] In the following, we shall show that a quantitative agreement can also be obtained for the nuclear-spin-relaxation rate. (The analysis of infrared conductivity will be given separately.)

## II. AMPLITUDES DUE TO BOSON CONTRIBUTION

Let $\mathbf{r}_1$ and $\mathbf{r}_2$ be the coordinates of $e_\uparrow$ and $e_\downarrow$ in the resonance state $\phi$, and

$$\frac{1}{\sqrt{\Omega}} e^{i\mathbf{q}\cdot\mathbf{r}_b} U(\mathbf{r}) \tag{2.1}$$

be its normalized orbital wave function, where

$$\mathbf{r}_b = \tfrac{1}{2}(\mathbf{r}_1+\mathbf{r}_2) \tag{2.2}$$

is the center-of-mass coordinate of the boson,

$$\mathbf{r} = \mathbf{r}_1 - \mathbf{r}_2 \tag{2.3}$$

the relative coordinate, and the normalization condition requires

$$\int |U(\mathbf{r})|^2 d^3 r = 1\ . \tag{2.4}$$

Thus, the total wave function (including spins) is $(2\Omega)^{-1/2} e^{i\mathbf{q}\cdot\mathbf{r}_b}$ times

$$U(\mathbf{r}) e_\uparrow(\mathbf{r}_1) e_\downarrow(\mathbf{r}_2) - U(-\mathbf{r}) e_\uparrow(\mathbf{r}_2) e_\downarrow(\mathbf{r}_1)\ .$$

On account of the quasi-two-dimensional nature of the crystal, this wave function is not isotropic. The Fourier component of $U(\mathbf{r})$ is

$$u(\mathbf{k}) \equiv \int U(\mathbf{r}) e^{i\mathbf{k}\cdot\mathbf{r}} d^3 r\ , \tag{2.5}$$

which satisfies

$$(8\pi^3)^{-1}\int |u(\mathbf{k})|^2 d^3k = 1 \ .$$

It is convenient to choose $U(\mathbf{r})$ real for even-parity states but imaginary for odd-parity ones; i.e., the complex conjugate of $U(\mathbf{r})$ satisfies

$$U(\mathbf{r})^* = U(-\mathbf{r}) \ , \tag{2.6}$$

and therefore

$$u(\mathbf{k})^* = u(\mathbf{k}) = \text{real} \ . \tag{2.7}$$

In order that the resonant state can be approximately represented by a local field operator $\phi(\mathbf{r})$, a necessary condition is for $u(\mathbf{k})$ to receive its main support from $\mathbf{k}$ vectors that are outside the Fermi surface; otherwise, the boson operators cannot (approximately) satisfy the required commutation relations, even for matrix elements between the low-lying states. Hence,

$$\overline{k^2} \equiv (8\pi^3)^{-1}\int u(\mathbf{k})^2 k^2 d^3k > k_F^2 \ . \tag{2.8}$$

In Fig. 1, all crosses denote the action of the contact Hamiltonian (1.6). Figure 1(a) represents the nuclear spin flip through its collision with a "free" electron:

$$e_\downarrow(\mathbf{p}_1) + I_z \to e_\uparrow(\mathbf{p}_2) + (I_z - 1) \ . \tag{2.9}$$

This gives an amplitude

$$-(1/3\Omega) I_- \gamma_e \gamma_N e^{i\mathbf{K}\cdot\mathbf{r}_N} \ , \tag{2.10}$$

where $\mathbf{K} = \mathbf{p}_1 - \mathbf{p}_2$ is the momentum transfer given to the nucleus. The boson-dissociation reaction (1.9) is represented by Figs. 1(b) and 1(c). In the "impulse" approximation, we neglect the final state interaction between the "free" electrons $e_\uparrow(\mathbf{p}_1)$ and $e_\uparrow(\mathbf{p}_2)$. As will be shown in remark (2) below, the sum of these two amplitudes, Figs. 1(b) and 1(c), is the product of (2.10) times

$$\mathcal{M}_{\mathbf{p}_1\mathbf{p}_2\mathbf{q}} = u(\mathbf{p}_2 - \mathbf{q}/2) - u(\mathbf{p}_1 - \mathbf{q}/2) \ , \tag{2.11}$$

where the minus sign between the two $u$ functions is due to the antisymmetry in the final two-electron wave function, and the momentum transfer $\mathbf{K}$ in (2.10) is now given by

$$\mathbf{K} = \mathbf{q} - \mathbf{p}_1 - \mathbf{p}_2 \ , \tag{2.12}$$

with $\mathbf{q}$ denoting the initial $\phi$ momentum. In deriving (2.11), we have made use of the reality condition (2.6). This condition is related to the convention for relative phase between the initial state $\phi$ and the final state $e_\uparrow(\mathbf{p}_1)e_\uparrow(\mathbf{p}_2)$; as we shall see, the same convention also determines the phase of the amplitude for the time-reversed reaction

$$e_\downarrow(-\mathbf{p}_1) + e_\downarrow(-\mathbf{p}_2) + I_z' \to \phi(-\mathbf{q}) + (I_z' - 1) \ , \tag{2.13}$$

where $I_z' = -(I_z - 1)$ and $I_z' - 1 = -I_z$. By relabeling $I_z'$ as $I_z$, we find the amplitude sum of Figs. 1(d) and 1(e) to be $-1$ times that of 1(b) and 1(c), as given by the second term in (1.10).

In accordance with (1.4), the top Fermi energy $\varepsilon_F$ is $\nu$ (at zero temperature). Assume the temperature $T$ is not too high, so that $k_B T \ll \varepsilon_F$, where $k_B$ is the Boltzmann constant. Thus, the magnitude of the $\phi$ momentum $\mathbf{q}$ is $\ll k_F$. Since the Zeeman splitting for the nuclear spin levels is only $\sim 10^{-6}$ times $\varepsilon_F$, energy conservation requires the relevant final momenta $\mathbf{p}_1$ and $\mathbf{p}_2$ in reaction (1.9) to lie near the Fermi surface; i.e., their magnitudes are $\cong k_F$. Hence, the nuclear-spin-relaxation rate due to boson dissociation (1.9), or to its inverse reaction (2.13), is proportional to $Gn_b$, where $n_b$ is the expectation value of the boson number operator (1.14) and $G$ is the angular average

$$G \equiv (4\pi)^{-2}\int d^2\hat{\mathbf{p}}_1 \int d^2\hat{\mathbf{p}}_2 |\mathcal{M}_{\mathbf{p}_1\mathbf{p}_2\mathbf{q}}|^2 \ ,$$

with $\mathbf{p}_1$ and $\mathbf{p}_2$ both on the surface of the Fermi sphere, and $\hat{\mathbf{p}}_1$, $\hat{\mathbf{p}}_2$ their corresponding unit vectors. Because $|\mathbf{q}| \ll k_F$, we can make the approximation of replacing $(\mathbf{p}_i - \frac{1}{2}\mathbf{q})$ by $\mathbf{p}_i$ in (2.11), where $i = 1$ or 2; hence, $G$ becomes $\mathbf{q}$ independent and is given by

$$G \cong (4\pi)^{-2}\int d^2\hat{\mathbf{p}}_1 \int d^2\hat{\mathbf{p}}_2 [u(\mathbf{p}_2) - u(\mathbf{p}_1)]^2 \ . \tag{2.14}$$

[See Eqs. (3.4) and (3.9)–(3.12) below for the precise use of $G$.]

To estimate the magnitude of $G$ we assume, as an example, the internal wave function $U(\mathbf{r})$ of $\phi$ to be a $p$ state

$$U(\mathbf{r}) = i\pi^{-1/2}\lambda^{5/2} z e^{-\lambda r} \ ; \tag{2.15}$$

its Fourier component (2.5) is

$$u(\mathbf{k}) = -2^5\pi^{1/2}\lambda^{7/2} k_z (k^2 + \lambda^2)^{-3} \ . \tag{2.16}$$

Thus, (2.14) gives $G \cong \frac{1}{3} 2^{11}\pi\lambda^7 k_F^2 (k_F^2 + \lambda^2)^{-6}$. The fermion number $n_f$ is related to $k_F$ by

$$n_f = (3\pi^2)^{-1} k_F^3 \ . \tag{2.17}$$

Multiplying $G$ by $n_f$ times $n_b/n_f$, we find

$$Gn_b \cong \frac{2^{11}}{9\pi} \frac{\lambda^7 k_F^5}{(k_F^2 + \lambda^2)^6} \frac{n_b}{n_f} \ . \tag{2.18}$$

From (2.8), we have

$$\overline{k^2} = \lambda^2 > k_F^2 \ . \tag{2.19}$$

At a given ratio $n_b/n_f$, the maximum of $Gn_b$ occurs at $\lambda^2 = 1.4 k_F^2$, which gives, for a $p$-state $\phi$ quantum, $(Gn_b)_{\max} \cong 1.23(n_b/n_f)$.

As another example, we may take the normalized $d$ wave

$$U(\mathbf{r}) = (2\pi)^{-1/2}\lambda^{7/2}(z^2 - r^2/3) e^{-\lambda r} \ , \tag{2.20}$$

which gives

$$u(\mathbf{k}) = \left[\frac{\pi}{2}\right]^{1/2} \frac{8^2\lambda^{9/2}}{(k^2 + \lambda^2)^4}(k^2 - 3k_z^2) \ , \tag{2.21}$$

$$\overline{k^2} = \lambda^2 > k_F^2 \ ,$$

and

$$Gn_b \cong \frac{(4k_F)^7\lambda^9}{15\pi(k_F^2+\lambda^2)^8}\frac{n_b}{n_f} . \tag{2.22}$$

At a given $n_b/n_f$, the maximum of $Gn_b$ is now $\cong 1.45(n_b/n_f)$, at $\lambda^2=9k_F^2/7$.

As remarked before, $\overline{k^2}=\lambda^2$ must be considerably larger than $k_F^2$, in order that the resonant state can be represented phenomenologically by an independent boson field $\phi(\mathbf{r})$. Take $\lambda=2k_F$ and for the above two examples we find

$$Gn_b=\begin{cases}0.593(n_b/n_f) & p \text{ wave} ,\\ 0.456(n_b/n_f) & d \text{ wave} .\end{cases} \tag{2.23}$$

At higher $\lambda$, $Gn_b$ decreases rapidly; e.g., at $\lambda=2.5k_F$, $Gn_b$ becomes $0.30(n_b/n_f)$ for the $p$ wave and $0.17(n_b/n_f)$ for the $d$ wave.

### Remarks

(1) In terms of $U(\mathbf{r})$, the boson operator $\phi$ can be expressed as a bilinear product of electron field operators $\psi$, introduced in (1.5):

$$\phi(\mathbf{r}_b)=\int d^3r U(\mathbf{r})\psi_\uparrow(\mathbf{r}_1)\psi_\downarrow(\mathbf{r}_2) , \tag{2.24}$$

where

$$\mathbf{r}_1=\mathbf{r}_b+\tfrac{1}{2}\mathbf{r} \quad\text{and}\quad \mathbf{r}_2=\mathbf{r}_b-\tfrac{1}{2}\mathbf{r} .$$

Under the (anti-unitary) time-reversal operator $T$, we define the phase factors $\eta_f$ and $\eta_b$ by

$$T\psi(\mathbf{r},t)T^{-1}=\eta_f\sigma_2\psi(\mathbf{r},-t)$$

and

$$T\phi(\mathbf{r},t)T^{-1}=\eta_b\phi(\mathbf{r},-t) , \tag{2.25}$$

where

$$\sigma_2=\begin{pmatrix}0 & -i\\ i & 0\end{pmatrix}$$

and $|\eta_f|^2=|\eta_b|^2=1$. The phase convention (2.6) and $T$ invariance lead to

$$\eta_b=-\eta_f^2 , \tag{2.26}$$

independent of the parity of $U(\mathbf{r})$.

Applying $T$ onto the annihilation operators $a_{\mathbf{p}\uparrow}$, $a_{\mathbf{p}\downarrow}$, and $b_\mathbf{p}$ defined by (1.7) and (1.12), we have

$$Ta_{\mathbf{p}\uparrow}T^{-1}=-i\eta_f a_{-\mathbf{p}\downarrow} ,$$
$$Ta_{\mathbf{p}\downarrow}T^{-1}=i\eta_f a_{-\mathbf{p}\uparrow}, \tag{2.27}$$

and

$$Tb_\mathbf{p}T^{-1}=\eta_b b_{-\mathbf{p}} .$$

Write the boson-fermion coupling interaction as

$$H_{\text{int}}=g\sum_{\mathbf{k}_1,\mathbf{k}_2}[v(\mathbf{k})b_\mathbf{q}^\dagger a_{\mathbf{k}_1\uparrow}a_{\mathbf{k}_2\downarrow}+v(\mathbf{k})^* a_{\mathbf{k}_2\downarrow}^\dagger a_{\mathbf{k}_1\uparrow}^\dagger b_\mathbf{q}] \tag{2.28}$$

with $g$ real,

$$\mathbf{k}_1=\tfrac{1}{2}\mathbf{q}+\mathbf{k}$$

and

$$\mathbf{k}_2=\tfrac{1}{2}\mathbf{q}-\mathbf{k} . \tag{2.29}$$

It can be readily verified that, on account of (2.26) and (2.27), $T$ invariance requires

$$v(\mathbf{k})^*=v(\mathbf{k})=\text{real} , \tag{2.30}$$

similar to (2.7).

Below the critical temperature $T_c$, the statistical ensemble average $\langle b_0\rangle$ for the zero-momentum boson operator $b_0$ is of a macroscopic amplitude:

$$\langle b_0\rangle=\Omega^{1/2}B , \tag{2.31}$$

where

$$B=|B|e^{i\gamma} \tag{2.32}$$

is the long-range order parameter that characterizes the Bose-Einstein condensation. As shown in Ref. 4, this induces the following transformation from the fermion operators $a_{\mathbf{p}\uparrow}$ and $a_{\mathbf{p}\downarrow}$ to the "quasiparticle" operators $\alpha_{\mathbf{p}\uparrow}$ and $\alpha_{\mathbf{p}\downarrow}$:

$$\alpha_{\mathbf{p}\uparrow}=a_{\mathbf{p}\uparrow}\cos\theta_\mathbf{p}-e^{i\gamma}a_{-\mathbf{p}\downarrow}^\dagger\sin\theta_\mathbf{p} ,$$
$$\alpha_{-\mathbf{p}\downarrow}=e^{i\gamma}a_{\mathbf{p}\uparrow}^\dagger\sin\theta_\mathbf{p}+a_{-\mathbf{p}\downarrow}\cos\theta_\mathbf{p} , \tag{2.33}$$

where

$$\sin 2\theta_\mathbf{p}=g|B|v(\mathbf{p})/E_\mathbf{p} ,$$
$$\cos 2\theta_\mathbf{p}=(p^2/2m_f-\mu)/E_\mathbf{p} , \tag{2.34}$$

$$E_\mathbf{p}=[(p^2/2m_f-\mu)^2+\Delta(\mathbf{p})^2] , \tag{2.35}$$

and the gap energy squared is

$$\Delta(\mathbf{p})^2=[g|B|v(\mathbf{p})]^2 . \tag{2.36}$$

These formulas will be used in the next section; their validity depends on $T$ invariance and the phase convention (2.6) and (2.7).

The effect of $\Delta(\mathbf{p})$ becomes most important when the fermion kinetic energy $(2m_f)^{-1}p^2$ is near the top Fermi energy $\mu$, which is, in turn $\cong \nu=\frac{1}{2}$ times the excitation energy $2\nu$ of the resonant $\phi$ state. Hence, we may approximate $v(\mathbf{p})$ as a function only of the unit vector $\hat{\mathbf{p}}=\mathbf{p}/p$. For the $p$-state wave function (2.16), we assume $v(\mathbf{p})\propto\hat{\mathbf{p}}_z$ and write

$$\Delta(\mathbf{p})^2=3\Delta_0^2\hat{\mathbf{p}}_z^{\,2} , \tag{2.37}$$

so that the angular average of $\Delta(\mathbf{p})^2$ is

$$\Delta_0^2\equiv|gB|^2 \tag{2.38}$$

[i.e., $v(\hat{\mathbf{p}})^2$ is normalized to have its angular average = 1]. Likewise for the $d$-state wave function (2.21), we have

$$\Delta(\mathbf{p})^2=\tfrac{5}{4}\Delta_0^2(1-3\hat{\mathbf{p}}_z^{\,2})^2 . \tag{2.39}$$

(2) The amplitude (2.10) and (2.11) for the reaction (1.9)

can be readily derived by evaluating the matrix element of the Fermi interaction $H$, given by (1.6), between the initial and final states: $|i\rangle = b^\dagger_{\mathbf{q}}|I_z\rangle$ and $|f\rangle = a^\dagger_{\mathbf{p}_1\uparrow}a^\dagger_{\mathbf{p}_2\uparrow}|I_z-1\rangle$, where $|I_z\rangle$ denotes the state with the nuclear $z$-component spin $I_z$, but without any boson or fermion. By using (1.7), (1.12), (2.24), and the phase convention (2.7), we find

$$\langle f|H|i\rangle = -\tfrac{1}{3}\Omega^{-3/2}\gamma_e\gamma_N I_- \mathcal{M}_{\mathbf{p}_1\mathbf{p}_2\mathbf{q}} e^{i(\mathbf{q}-\mathbf{p}_1-\mathbf{p}_2)\cdot\mathbf{r}_N} , \tag{2.40}$$

where $\mathcal{M}_{\mathbf{p}_1\mathbf{p}_2\mathbf{q}}$ is given by (2.11).

Similarly, for the time-reversed reaction (2.13), the initial state is $|i\rangle = a^\dagger_{-\mathbf{p}_1\downarrow}a^\dagger_{-\mathbf{p}_2\downarrow}|I_z\rangle$, and the final state $|f\rangle = b^\dagger_{-\mathbf{q}}|I_z-1\rangle$; the corresponding matrix element $\langle f|H|i\rangle$ is $-1$ times (2.40). This then establishes the minus sign inside the parenthesis of the last term in (1.10).

(3) The condition (2.8) is necessary for the approximation that $\psi_f(\mathbf{r})$ and $\phi(\mathbf{r})$, given by (1.7) and (1.12), can be regarded as independent field operators. Clearly, this approximation breaks down if the boson momentum $\mathbf{q}$ is sufficiently high, so that either $\mathbf{q}/2+\mathbf{k}$ or $\mathbf{q}/2-\mathbf{k}$ (denoting one of the momenta of the "bound" electrons inside the resonant boson state) may lie within the Fermi sea, even if $k > k_F$.

(4) There are strong dynamical reasons, due to the interaction between $\phi$ and the lattice sites, to restrict further the magnitude of the boson momentum. In the $s$-channel theory, the boson is an excited resonant state; by itself, it is unstable with an excitation energy $2\nu$ in the rest frame [as shown in (1.3)]. This instability would increase when the boson is in motion, because of collisions with lattice sites. Therefore, its density of states $\rho_b(\omega)d\omega$ for a kinetic energy between $\omega$ and $\omega+d\omega$ should be less than that of the free particles, especially when $\omega$ is large. In the following we assume

$$\rho_b(\omega) = \frac{m_b^{3/2}\omega^{1/2}}{\sqrt{2}\pi^2}\left(e^{(\omega-\omega_c)/D}+1\right)^{-1} , \tag{2.41}$$

where $\omega_c$ and $D$ are two real positive parameters to be determined phenomenologically by experiment. As we shall see, $\omega_c$ is $>>D$. Hence, the reduction factor $(e^{(\omega-\omega_c)/D}+1)^{-1}$ is near 1 when $\omega$ is small; it becomes $\frac{1}{2}$ at $\omega=\omega_c$, decreases rapidly over a width $O(D)$, and approaches 0 when $\omega\to\infty$.

## III. RELAXATION RATES

### A. Normal phase

According to the effective Hamiltonian (1.10), in the normal phase there are three incoherent processes contributing to reaction (1.8), as shown in Fig. 1. The rate for each process is obtained from the standard expression

$$R = 2\pi\sum_{i,f}|\langle f|H_{\text{eff}}|i\rangle|^2 w(E_f,E_i)\delta(E_f-E_i) , \tag{3.1}$$

where $|i\rangle$ and $|f\rangle$ are the initial and final states, $E_i$ and $E_f$ are the initial and final energies of the electron system, and $w(E_f,E_i)$ is the appropriate product of fermion or boson distribution functions. The nuclear-spin energy has been neglected in (3.1), since it is much smaller than any other energy involved.

For the process due to free electrons [Fig. 1(a)], the rate is simply given by

$$R_1 = (\pi/18)\gamma_e^2\gamma_N^2 I_-^2\rho_f^2\int_{-\infty}^{\infty}d\varepsilon f(\varepsilon)[1-f(\varepsilon)] , \tag{3.2}$$

where $\rho_f = \sqrt{2}m_f^{3/2}\varepsilon_F^{1/2}/\pi^2$ is the density of states at the Fermi surface (including both spins) and

$$f(\varepsilon) = \frac{1}{e^{\beta\varepsilon}+1}$$

is the fermion distribution function where $\beta = 1/k_BT$ and $\varepsilon = p^2/2m_f - \mu$ with $\mu$ the Gibbs chemical potential. The integration over $\varepsilon$ is elementary and the result is

$$R_1 = (\pi/18)\gamma_e^2\gamma_N^2 I_-^2\rho_f^2 k_BT . \tag{3.3}$$

It follows that $R_1/T$ is independent of the temperature; this is known as the Korringa law.[8]

For the process involving bound electrons [Figs. 1(b) and 1(c)], the rate reads

$$R_2 = \frac{\pi}{36}G\gamma_e^2\gamma_N^2 I_-^2\rho_f^2\int_0^{\infty}d\omega\,\rho_b(\omega)g(\omega)\int_{-\infty}^{\infty}d\varepsilon[1-f(\varepsilon)][1-f(\omega+2(\nu-\mu)-\varepsilon)] , \tag{3.4}$$

where

$$g(\omega) = \frac{1}{\zeta^{-1}e^{\beta\omega}-1}$$

is the boson distribution function with a fugacity $\zeta = \exp[2\beta(\mu-\nu)]$ and $\rho_b(\omega)$ is the density of states of bosons given by (2.41). The fermionic integration in (3.4) can be worked out explicitly, yielding

$$R_2 = \frac{\pi}{36}G\gamma_e^2\gamma_N^2 I_-^2\rho_f^2 \times\int_0^{\infty}d\omega\rho_b(\omega)\frac{\zeta[\omega-(1/\beta)\ln\zeta]e^{-\beta\omega}}{(1-\zeta e^{-\beta\omega})^2} . \tag{3.5}$$

For bosons with a free particle density of states [$\omega_c\to\infty$ in (2.41)], the rate at the critical temperature is given by

$$R_2 = \tfrac{3}{4}Gn_bR_1 ,$$

where $n_b$ is boson density.

The electron part of the processes in Figs. 1(d) and 1(e) is the inverse of that of the processes in 1(b) and 1(c); the corresponding rate is equal to (3.4) after neglecting the nuclear magnetic energy. The total rate in the normal phase is then

$$R_n = R_1 + 2R_2 . \tag{3.6}$$

### B. Superconducting phase

To obtain the rate of reaction (1.8) in the superconducting phase, the effective Hamiltonian (1.10) has to be expressed in terms of the long-range order $B$ and the quasiparticle operators, $\alpha_{\mathbf{p}\sigma}$ and $\alpha^\dagger_{\mathbf{p}\sigma}$ ($\sigma=\uparrow$ and $\downarrow$) introduced in (2.32) and (2.33). The resultant Hamiltonian is

$$H_{\rm eff}=-\frac{1}{6\Omega}\gamma_e\gamma_n I_-\sum_{\mathbf{p}_1,\mathbf{p}_2}\Bigg\{-(e^{i\gamma}\alpha^\dagger_{\mathbf{p}_2\uparrow}\alpha^\dagger_{-\mathbf{p}_1\uparrow}-e^{-i\gamma}\alpha_{-\mathbf{p}_2\downarrow}\alpha_{\mathbf{p}_1\downarrow})\sin(\theta_{\mathbf{p}_2}-\theta_{-\mathbf{p}_1})+2\alpha^\dagger_{\mathbf{p}_2\uparrow}\alpha_{\mathbf{p}_1\downarrow}\cos(\theta_{\mathbf{p}_2}-\theta_{-\mathbf{p}_1})$$
$$+|B|\mathcal{M}_{-\mathbf{p}_1,\mathbf{p}_2,0}[(e^{i\gamma}\alpha^\dagger_{-\mathbf{p}_1\uparrow}\alpha^\dagger_{\mathbf{p}_2\uparrow}-e^{-i\gamma}\alpha_{-\mathbf{p}_2\downarrow}\alpha_{\mathbf{p}_1\downarrow})\cos(\theta_{\mathbf{p}_2}-\theta_{-\mathbf{p}_1})+2\alpha^\dagger_{\mathbf{p}_2\uparrow}\alpha_{\mathbf{p}_1\downarrow}\sin(\theta_{\mathbf{p}_2}-\theta_{-\mathbf{p}_1})]$$
$$+\frac{1}{\sqrt{\Omega}}\sum_{\mathbf{q}}\mathcal{M}_{-\mathbf{p}_1,\mathbf{p}_2,\mathbf{q}}[b_{\mathbf{q}}(\alpha^\dagger_{-\mathbf{p}_1\uparrow}\alpha^\dagger_{\mathbf{p}_2\uparrow}\cos\theta_{\mathbf{p}_2}\cos\theta_{-\mathbf{p}_1}+e^{-2i\gamma}\alpha_{\mathbf{p}_1\downarrow}\alpha_{-\mathbf{p}_2\downarrow}\sin\theta_{\mathbf{p}_2}\sin\theta_{-\mathbf{p}_1}$$
$$-2e^{-i\gamma}\alpha^\dagger_{\mathbf{p}_2\uparrow}\alpha_{\mathbf{p}_1\downarrow}\cos\theta_{\mathbf{p}_2}\sin\theta_{-\mathbf{p}_1})$$
$$-b^\dagger_{-\mathbf{q}}(e^{2i\gamma}\alpha^\dagger_{\mathbf{p}_2\uparrow}\alpha^\dagger_{-\mathbf{p}_1\uparrow}\sin\theta_{\mathbf{p}_2}\sin\theta_{-\mathbf{p}_1}+\alpha_{-\mathbf{p}_2\downarrow}\alpha_{\mathbf{p}_1\downarrow}\cos\theta_{\mathbf{p}_2}\cos\theta_{-\mathbf{p}_1}$$
$$-2e^{i\gamma}\alpha^\dagger_{\mathbf{p}_2\uparrow}\alpha_{\mathbf{p}_1\downarrow}\sin\theta_{\mathbf{p}_2}\cos\theta_{-\mathbf{p}_1})]\Bigg\}\,, \tag{3.7}$$

where $\theta_{\mathbf{p}}$ is given by (2.34).

All the processes contributing to reaction (1.8) in the superconducting phase are shown in Fig. 2 with $e'$ denoting a quasiparticle and $e$ a real particle. Their rates are given below.

(1) Direct quasiparticle "scattering" [Fig. 2(a), the process in the BCS theory]:

$$R_1=\frac{2\pi}{9}\gamma_e^2\gamma_N^2 I_-^2\int\frac{d^3p_1}{(2\pi)^3}\int\frac{d^2p_2}{(2\pi)^3}\cos^2(\theta_{\mathbf{p}_2}-\theta_{-\mathbf{p}_1})f(E_1)[1-f(E_2)]\delta(E_2-E_1)$$
$$=\frac{\pi}{9}\gamma_e^2\gamma_N^2 I_-^2\rho_f^2\int_0^\infty dE\,[E^2\chi_0^2(E)+\Delta_0^2\chi_1^2(E)]\frac{e^{-\beta E}}{(1+e^{-\beta E})^2}\,, \tag{3.8}$$

where $\chi_0(E)$ and $\chi_1(E)$ are defined by (3.10) below.

(2) Quasiparticle "scattering" due to the bound electrons inside the condensed (zero-momentum) bosons [Figs. 2(b) and 2(c)]:

$$R_2^{(0)}=\frac{2\pi}{9}\gamma_e^2\gamma_N^2 I_-^2|B|^2\int\frac{d^3p_1}{(2\pi)^3}\int\frac{d^3p_2}{(2\pi)^3}|\mathcal{M}_{-\mathbf{p}_1,\mathbf{p}_2,0}|^2\sin^2(\theta_{\mathbf{p}_2}-\theta_{-\mathbf{p}_1})f(E_1)[1-f(E_2)]\delta(E_2-E_1)$$
$$=\frac{\pi G}{9}\gamma_e^2\gamma_N^2 I_-^2\rho_f^2|B|^2\int_0^\infty dE\{E^2[\chi_0(E)\chi_2(E)-\chi_1^2(E)]-\Delta_0^2[\chi_1(E)\chi_3(E)-\chi_2^2(E)]\}\frac{e^{-\beta E}}{(1+e^{-\beta E})^2}\,. \tag{3.9}$$

The functions $\chi_n(E)$, ($n=0,1,2,3$) in the above expressions result from the integrations over $\hat{\mathbf{p}}_{1z}$ and $\hat{\mathbf{p}}_{2z}$ and are given by

$$\chi_n(E)\equiv\frac{1}{2}\int_{-1}^{1}dx\frac{p^n(x)}{\sqrt{E^2-\Delta_0^2p^2(x)}}\Theta(E^2-\Delta_0^2p^2(x))\,, \tag{3.10}$$

where

$$p(x)=\begin{cases}\sqrt{3}x, & \text{for } p \text{ wave}\\ (\sqrt{5}/2)(3x^2-1), & \text{for } d \text{ wave}\,,\end{cases}$$

and the step function $\Theta$ restricts the integration within the interval where $E^2-\Delta_0^2p^2(x)$ is positive. Note that for $p$ wave, $\chi_1(E)=\chi_3(E)=0$.

(3) Quasiparticle "pair creation" due to the bound electrons inside the excited bosons, i.e., bosons with nonzero momenta, shown in Figs. 2(d) and 2(e):

$$R_2^{(1)}=\frac{\pi}{9}\gamma_e^2\gamma_N^2 I_-^2\int_0^\infty d\omega\,\rho_b(\omega)g(\omega)\int\frac{d^3p_1}{(2\pi)^3}\int\frac{d^3p_2}{(2\pi)^3}|\mathcal{M}_{\mathbf{p}_1,\mathbf{p}_2,\mathbf{q}}|^2\cos^2\theta_{\mathbf{p}_1}\cos^2\theta_{\mathbf{p}_2}$$
$$\times[1-f(E_1)](1-f(E_2)]\delta(E_2+E_1-\omega)$$
$$=\frac{\pi G}{72}\gamma_e^2\gamma_N^2 I_-^2\rho_f^2\int_0^\infty d\omega\,\rho_b(\omega)g(\omega)\int_0^\omega dE\,E(\omega-E)[\chi_0(E)\chi_2(\omega-E)+\chi_0(\omega-E)\chi_2(E)-2\chi_1(E)\chi_1(\omega-E)]$$
$$\times[1-f(E)][1-f(\omega-E)]\,. \tag{3.11}$$

(4) Quasiparticle "scattering" due to the bound electrons inside the excited boson [Figs. 2(f) and 2(g)]:

$$R_2^{(2)} = \frac{2\pi}{9}\gamma_e^2\gamma_N^2 I_-^2 \int_0^\infty d\omega\,\rho_b(\omega)g(\omega)\int\frac{d^3p_1}{(2\pi)^3}\int\frac{d^3p_2}{(2\pi)^3}|\mathcal{M}_{-\mathbf{p}_1,\mathbf{p}_2,\mathbf{q}}|^2\sin^2\theta_{-\mathbf{p}_1}\cos^2\theta_{\mathbf{p}_2}f(E_1)[1-f(E_2)]\delta(E_2-E_1-\omega)$$

$$= \frac{\pi G}{36}\gamma_e^2\gamma_N^2 I_-^2\rho_f^2\int_0^\infty d\omega\,\rho_b(\omega)g(\omega)\int_0^\infty dE\,E(E+\omega)[\chi_0(E)\chi_2(E+\omega)+\chi_0(E+\omega)\chi_2(E)-2\chi_1(E)\chi_1(E+\omega)]$$

$$\times f(E)[1-f(E+\omega)]\ . \qquad (3.12)$$

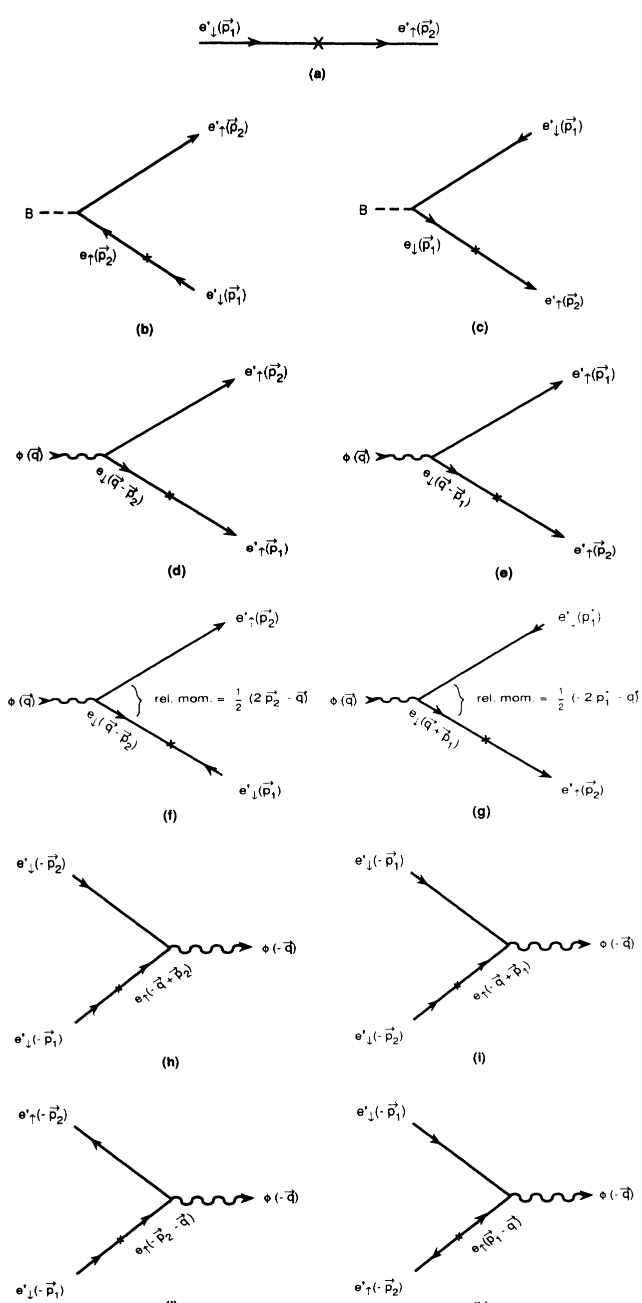

FIG. 2. All the processes contributing to reaction (1.8) in the superconducting phase, where $e'_\sigma(\mathbf{p})$ denotes a quasiparticle of momentum $\mathbf{p}$ and spin $\sigma$ $(=\uparrow,\downarrow)$, $B$ denotes the Bose condensate amplitude, $\phi(\mathbf{q})$ denotes a boson of nonzero momentum $\mathbf{q}$, and the cross represents the action of the contact interaction (1.6). The rates of these processes are given by (3.8)–(3.13).

The total rate in the superconducting phase is

$$R_s = R_1 + R_2^{(0)} + 2(R_2^{(1)} + R_2^{(2)})\ , \qquad (3.13)$$

where the factor 2 in the last term is due to the time-reversed processes of (3) and (4), as shown in Figs. 2(h)–2(k). The low-temperature behaviors of these processes can be obtained easily and are given by $R_1 \propto T^3$, $R_2^{(0)} \propto T^5$, and both $R_2^{(1)}$ and $R_2^{(2)} \propto T^{13/2}$. These results are quite different from the exponential suppression of the $s$-wave pairing model, since the gap energy in the pairing model with a *nonzero* orbital angular momentum vanishes in certain directions. For an arbitrary temperature below $T_c$, the integrals in (3.8)–(3.12) can be carried out numerically and the results will be discussed in the next section.

The total rate for reaction (1.8) being known, the nuclear-spin-relaxation rate $T_1^{-1}$ follows from the standard formula[8]

$$\frac{1}{T_1} = \frac{1}{2}\frac{\sum_{m,n} R_{mn}(E_m - E_n)^2}{\sum_n E_n^2}\ , \qquad (3.14)$$

where $R_{mn}$ is the transition rate from the nuclear spin $I_z = m$ to $I_z = n$, and $E_n$ is the nuclear-spin energy at $I_z = n$. In the problem being studied, only transitions $m - n = \pm 1$ are realized with the upper sign corresponding to reaction (1.8) and the lower sign to the reciprocal one.

## IV. RESULTS

The nuclear-spin-relaxation rates $T_1^{-1}$ at both the oxygen sites and at the copper sites of $YBa_2Cu_3O_{7-y}$ have been measured by a number of groups.[1,2] There are two striking features. One is the absence, in the superconducting phase, of the coherence peak that would be expected according to the standard BCS theory with an $s$-wave pairing state. The other is the decrease, in the normal phase, of the Korringa product $(TT_1)^{-1}$ at Cu sites with increasing temperatures. As will be explained below, both features are consistent with the boson-fermion model.

In Fig. 3, we plot the experimental values of the Korringa product from the measurement of Hammel *et al.*[1] and the numerical values of the Korringa product calculated from the boson-fermion model with a $p$-wave pairing state [Fig. 3(a)], and with a $d$-wave pairing state [Fig. 3(b)]. The open circles (O sites) and triangles (Cu sites) refer to the experimental data, and the solid circles (O sites) and triangles (Cu sites) are the theoretical values; the overall agreement is reasonably good. In these calcu-

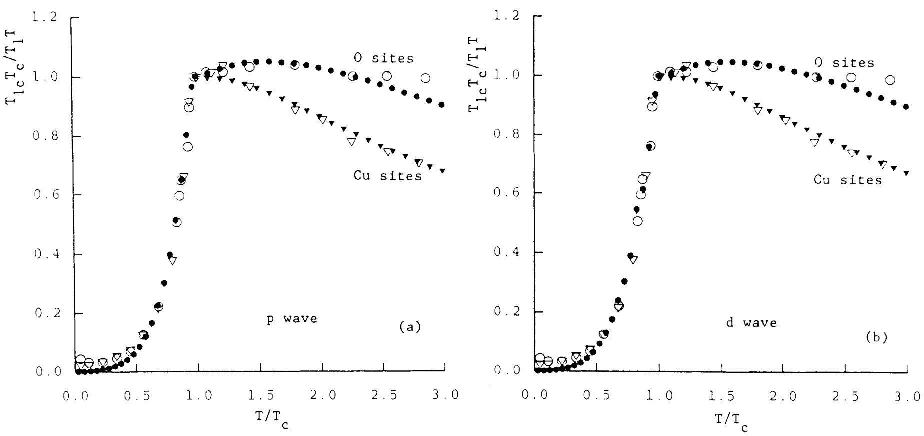


FIG. 3. Comparison between the Korringa product $(T_1T)^{-1}$ (in units of its value at the critical temperature $T_c$) measured experimentally and that calculated from the boson-fermion model with a $p$-wave pairing state, (a), and with a $d$-wave pairing state, (b). The open circles denote the experimental data at O sites and the solid circles denote the corresponding theoretical values. The open triangles denote the experimental data at Cu sites and the solid triangles denote the corresponding theoretical values.

lations, as an approximation, the chemical potential of bosons in the superconducting phase is set to zero and the temperature dependence of the Bose condensate is assumed to be that of an ideal Bose gas. The chemical potential in the normal phase is determined by the total density of particles. For the theoretical values in Fig. 3, we choose the parameters $\nu$($\frac{1}{2}$ of the resonance energy of the boson)$=5\kappa T_c$, $n_f=n_\nu\equiv(3\pi^2)^{-1}(2m_f\nu)^{3/2}$, and $n_b=3.5n_\nu$. These parameters are consistent with those determined from the application of the boson-fermion model to the Hall number measurement.[5] In addition, we set $\Delta_0(T=0)=3\kappa T_c$ for $p$ wave and $\Delta_0(T=0)=2.8\kappa T_c$ for $d$ wave, and $Gn_b=1$. The theoretical curves are rather insensitive to the parameters $\nu$, $n_b/n_f$, and $Gn_b$, even if they vary as much as 50% (the value of $Gn_b$, in particular, can be as large as 2 instead of 1). Only the Korringa product in the normal phase is sensitive to the parameters $\omega_c$ and $D$. In Fig. 3, we set

$$\omega_c=6\kappa T_c,\quad D=2\kappa T_c,\quad \text{for O sites}$$

and

$$\omega_c=3.5\kappa T_c,\quad D=0.1\kappa T_c,\quad \text{for Cu sites}\ .$$

Phenomenologically, this means more bosons at O sites than Cu sites. With these parameters, the ratio of the decay rate of a static boson in vacuum to the resonance energy of the boson turns out to be about 0.1, which can be regarded as the square of the dimensionless boson-fermion coupling parameter; this justifies the perturbative approximation we made in the superconducting phase. In the normal phase, the exact fermionic density-of-state function is used in the computation.

In the superconducting phase, the coherence peak can be diminished by smearing the density of states of the quasiparticles at the gap energy. This can be realized within the BCS theory if the pairing state is not $s$ wave, but $p$, $d$, or other higher-order partial waves, as was suggested for the heavy-fermion superconductors.[9] In the boson-dissociation processes [Figs. 2(f) and 2(g)], the integration over the boson energy naturally smears out the density of states of the quasiparticles even with an $s$-wave pairing state. With a pure $s$-wave pairing state, however, the $G$ factor defined in (2.14) will be too small to make the boson process dominant. Therefore, the nonzero orbital angular momentum component in the pairing state is required for both BCS and the boson-fermion model to explain the experimental results of the Korringa product in the superconducting phase. If the pairing state is a pure $p$ wave or $d$ wave, the experimental results can be fitted by both models. Only if the pairing state is a mixture of $s$ wave and other partial waves, say $s$-$d$ mixing, is the boson-fermion model preferred. In this case, the fermion process still exhibits the coherence peak on account of the nonzero gap energy generated by the $s$-wave component. However, in the boson-fermion model, because of boson dominance and because there is no coherence peak in boson-induced spin-flip processes, the agreement with experimental data in the superconducting phase can still be maintained.

In the normal phase, the decrease of the Korringa product on the Cu sites with increasing temperature is very hard to explain within the framework of a single Fermi sea of electrons. With the additional boson component, the situation is changed. The temperature-dependence of the Korringa product due to bosons is quite different from that due to fermions. Furthermore, a moving boson can decay through collisions with the lattice, and the decay rate may also be different at O sites from that at Cu sites since the size of a boson is comparable to the lattice spacing. Indeed, by assuming the bosonic density of states to be given by (2.41), we find that the Korringa product given by the processes in Figs. 1(b) and 1(c) decreases at higher temperature. With the choices of parameters $\omega_c$ and $D$ given above, a reasonably good fit of the experimental data in the normal phase can be obtained. This shows that, at least phenomenologically, the experimental results are consistent with the existence of the boson component.

## ACKNOWLEDGMENTS

We wish to thank Zhao-bing Su for discussions. This research was supported in part by the U.S. Department of Energy under Contract Nos. DE-AC02-76 ER02271 and DE-AC02-87 ER40325, Task B.

[1]P. C. Hammel *et al.*, Phys. Rev. Lett. **63**, 1992 (1989).

[2]For other experimental results of NMR, see, e.g., C. H. Pennington and C. P. Slichter, in *Physical Properties of High Temperature Superconductors,* edited by D. M. Ginsberg (World Scientific, Singapore, 1990).

[3]M. Tinkham, *Introduction to Superconductivity* (McGraw-Hill, New York, 1965).

[4]R. Friedberg and T. D. Lee, Phys. Lett. A **138**, 423 (1989); Phys. Rev. B **40**, 6745 (1989); R. Friedberg, T. D. Lee, and H. C. Ren, *ibid.* **42**, 4122 (1990).

[5]R. Friedberg, T. D. Lee, and H. C. Ren, Phys. Lett. A **152**, 417 (1991); **152**, 423 (1991).

[6]P. Chaudhari *et al.*, Phys. Rev. B **36**, 8903 (1987).

[7]R. T. Collins *et al.*, Phys. Rev. B **43**, 8701 (1991).

[8]C. P. Slichter, *Principles of Magnetic Resonance* (Springer-Verlag, Berlin, 1989).

[9]Y. Kitaoka *et al.*, J. Magn. Magn. Mater. **52**, 351 (1985).